JP&M Engineering
Journal of Petroleum and Mining Engineering

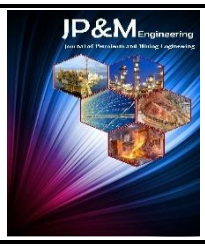

Spectrum of Hydrocarbon Contaminated Soil in North-West Suez Gulf of Egypt

Mostafa.M. Atwa[a*], Ayman. Hamed[b], Asmaa.H. Mohammed[c], Fares.I.A. Khedr[d] and Maher.A. Mesbah[b]

[a] Petroleum & LNG Inspector at Bureau Veritas

[b] Faculty of Petroleum and Mining Engineering, Suez University, Egypt

[c] Marine Sciences Department, National Authority for Remote Sensing and Space Sciences, (NARSS), Cairo 11769, Egypt

[d] Department of Geology, Faculty of Science, Suez University, Suez,43518, Egypt

*Corresponding author e-mail: ayman.hamed@suezuni.edu.eg

Article Info

Received 4 May 2023
Revised 1 Mar. 2024
Accepted 13 Mar. 2024

Keywords

"Oil spills; Contaminated soil; Sentinel-2; Gulf of Suez; Egypt"

Abstract

Oil spills are one of the major environmental challenges affecting urban coastal cities globally. A critical industrial area, known as El-Suez refining plant, located in the Suez city in the northwestern Gulf of Suez, was chosen as a case study.
Therefore, this study aims to detect spatial-temporal contaminated soil from oil seepage events to understand the role of human activities and the physical condition of the study area. This was achieved using maximum likelihood classification, using multi-spectral satellite data of Sentinel-2 integrated with field sampling and previous studies on the same area. Analyzing Sentinel-2 data from 2015 to 2021 revealed a potential increase in contamination, coinciding with darker areas observed in the images. Additionally, spectral reflectance analysis confirmed the presence of hydrocarbons, with the 1700nm wavelength being the most reliable for detection. The resulting Land use Land cover (LU-LC) shows acceptable accuracy, with 83.33% overall and 80% for detecting contaminated soil, showcasing its potential for large-scale monitoring. The study successfully identified contaminated areas near pipelines and deactivated land farms, suggesting past bioremediation attempts. This study can be applied in similar areas to mitigate the oil spills from storage tanks and oil transfer pipelines, enhancing the environmental management strategy of oil pollution.

Introduction

Hydrocarbon micro-seepage is a common environmental issue occurring due to onshore oil tanks and transferring pipelines in urban coastal areas. Oil spills, when they occur in this environment, display a different spectral appearance that distinguished them from the surrounding land covers. Usually oil spills with the presence of characterized by the abnormal natural surface spectral landscape characteristics of mineral alteration features and geobotanic anomalies like formatting dark spots that can be detected by satellite imagery [1]. Multispectral remote sensing, i.e., Landsat and Sentinel-2, stands out as a vigorous technology, offering cost-effective spatiotemporal monitoring of contaminated soils compared to traditional methods [2].

Traditional soil assessment methods often rely on raster sampling, necessitating numerous sample collections and intricate laboratory procedures like separation and preconcentration [3]. This can be burdensome for large-scale mapping of contaminated areas. Therefore, there's a growing demand for faster, environmentally friendly, and cost-effective sensing technologies. Fortunately, these modern techniques offer significant advantages over their predecessors, including portability, rapid data acquisition, broader detection ranges for elements, minimal sample preparation needs, and user-friendly operation [4].

By utilizing proximal and remote sensing technologies, we can gain valuable insights for both pollution detection and ecological risk monitoring [5]. [6] conducted research using multi-temporal Landsat imagery scenes to study the quantity of polluted area at Burgan Oil field, Kuwait. They used algorithms to estimate Land Surface Temperatures (LST) from emitted radiance to detect contaminated areas and correlate them with polluted areas at field. Using electromagnetic radiation for collecting information of an object or phenomenon without physical contact is the definition of remote sensing according to [7] as well as [8].

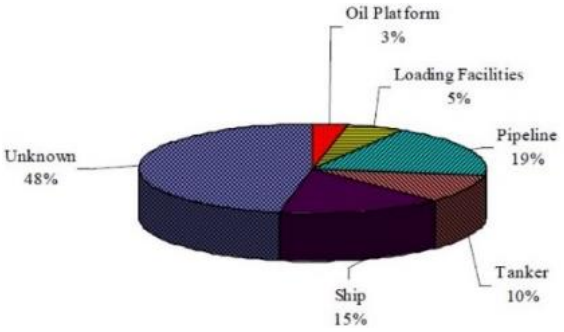

Figure 1 Sources of spilled oil in Suez Gulf [9].

[10] used WorldView-3 super spectral satellite images for direct hydrocarbons detection in contaminated soils. The study utilized multiple datasets of spectral signatures libraries collected from several simulation experiments; data of hyperspectral imaging instrument for distinctive hydrocarbons measured in the laboratory and an imagery acquired by airborne instrument with VNIR and SWIR bands. In addition to WV-3 data. It was clear that hydrocarbons absorption feature in WV-3's band 12 is resilient enough and persists under various conditions to detect contaminated soils with hydrocarbons.

While both (Sentinel-2 and Landsat-8) offer multispectral data, Sentinel-2 boasts a higher spatial resolution (10m vs. 30m for Landsat 8), enabling precise characterization of individual refinery features like storage tanks and potential leakage zones. Furthermore, Sentinel-2's inclusion of red-edge and near-infrared bands facilitated accurate differentiation between healthy and potentially contaminated vegetation, crucial for our assessment of environmental impacts [11]. Finally, the 5-day revisit time of Sentinel-2 compared to Landsat 8's 16-day revisit time allowed for more frequent monitoring of potential temporal changes in the refinery operations and its environmental dynamics. Therefore, Sentinel-2 satellite imagery was chosen due to its superior capabilities compared to Landsat. This combination of enhanced spatial resolution, targeted spectral bands, and improved temporal resolution made Sentinel-2 the optimal choice for our comprehensive study of the hydrocarbon refining plant in urban coastal areas.

In Egypt, according to the data from the Environmental Management Units (EMU's) of Suez Governorate, the total number of vessels passing through Suez Canal amounts to 16,000 vessels every year, with transferring around 125 million tons of oils and oil products yearly. Besides, approximately 3,000 vessels sail to ports located in Suez. Tanker vessels are considered the main source of oil pollution offshore. Regional environmental management improvement project reports released in July 2008 powered by Japan International Cooperation Agency (JICA), mentioned that 19% of spilled oil in Gulf of Suez area caused by the breakdown or wrong operations in pipelines or storage tanks (Figure 1). Onshore oil spills, if not promptly addressed, can pose significant environmental and socioeconomic threats. Contamination of soil and groundwater can harm sensitive ecosystems and disrupt agricultural activities. Furthermore, oil spills can negatively impact coastal resources, affecting fisheries and tourism, vital sectors for the local economy.

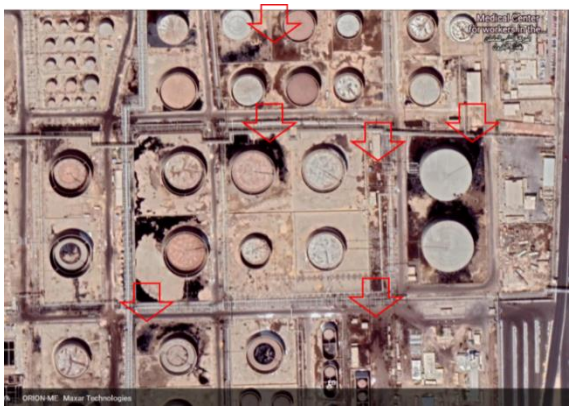

Figure 2 Airborne image of El Suez refinery plant area generated by google earth, showing dark spots inside studied area.

Consequently, El-Suez refinery plant, located in northwestern Gulf of Suez, was chosen as a case study. Suez governorate houses six industrial zones, encompassing diverse industries, notably 26 oil-related enterprises. Among these: El Nasr Petroleum company and Suez Oil Processing company both of them produce various petroleum derivatives (asphalt, kerosene, gasoline). Darker areas near their tanks (Figure 2) potentially indicate prior hydrocarbon spills. The targeted companies holding a prominent position in Egypt's refining sector, they are not only processes oil but also stores exported products in extensive tanks. Additionally, SAVOLA operates in food oil production with compliant wastewater treatment, while CALTEX, CO-OPERATION, ESSO, and MISR PETROLEUM provide marine fuelling services from El-Zaytyat Port storage facilities [9].

To this end, the aim of study is to monitor spatiotemporal hydrocarbon contaminated soil using Sentinel-2 between 2015 and 2021 in urban costal area.

Study Area

The survey was carried out at two Suez refinery companies located between 29° 59' 30" N 32° 27' 0" and 29° 55' 30" N, 32° 34' 0" E, at the western top of the Gulf of Suez shoreline as shown in (Figure 3). The chosen study area comprises Suez Oil Processing Company and El-Nasr Petroleum Company, represents a significant hub for oil operations within Egypt. The heavily industrial activities including oil refining, storage, and transportation, while contributing to the region's economy, also entails inherent risks of environmental contamination, particularly through potential oil spills onshore [12]. For example, the combined processing capacity of these companies approximately 68,000 barrels per day (BOPD). Moreover, the presence of El Nasr Petroleum Company further expands the range of petroleum derivatives produced and handled within the vicinity. Additionally, numerous companies

Figure 3 Geographic location of the studied area.

like Misr and CO-OPERATION operate storage tanks adjacent to El-Zaytyat Port for marine vessel fueling.

With such a dense concentration of oil infrastructure and operations, the potential of onshore spills arises from various sources. Various unexpected events, including leaks from aging pipelines, storage tank malfunctions, human error during transportation, and even accidents during refinery operations, can all contribute to oil releases onto land. Studies have highlighted the vulnerability of coastal areas to onshore spills, emphasizing the need for robust containment and mitigation strategies ([13]; [14]; [15]).

Data Collections and Methods:

The field ground truthing points were collected in the soil contamination areas within the Suez refinery plant (Figure 4). The location of samples was stored using GPS device to be used in extracting spectral signatures from satellite images for related soil contaminated class, as shown in (Figure 5). Initially we observed contamination levels at five points around the Suez Refinery Plant (Table 1). Two points inside the plant represented low and heavy contamination, while three points outside represented clear soil, soil with groundwater contamination, and soil near buildings.

Table 1 Coordinates of some reference points

Point	Longitude	Lattitude
Light Contaminated	32.50059591	29.96106377
Heavy Contaminated	32.49980907	29.9622825
G-water	32.50842699	29.95625559
Clear	32.51810818	29.95475434
Buildings	32.51928045	29.96272939

Then we repeated this method using optical observation of contamination and previous studies on the same area to get more reference points. These points are reassigned on aerial image to be used as dataset to generate Region of Interest (ROI's). Choosing pure ROIs from field georeferencing *in situ* point for every feature on satellite images then extracted the values from image pixels and integrated to be used in classification method using ENVI program.

Figure 4 Showed ground truthing points on green colour located on Sentinel-2 image.

The current study utilized two different satellite image datasets. The first dataset consisted of Sentinel-2 images with varying spatial resolutions (10m, 20m, and 60m) covering the Suez governorate region. Sentinel-2A and Sentinel-2B satellites provide data in 13 bands through their Multispectral Instruments (MSI). Level-1C products, offering ortho-rectified top-of-atmosphere reflectance, were downloaded from the USGS website and used from 2015 to 2021. The second dataset included Planetscope imagery with four visible and near-infrared spectral bands at 3-meter pixel resolution. This dataset was acquired on October 21, 2021, through collaboration with NARSS (National Authority for Remote Sensing and Space Science).

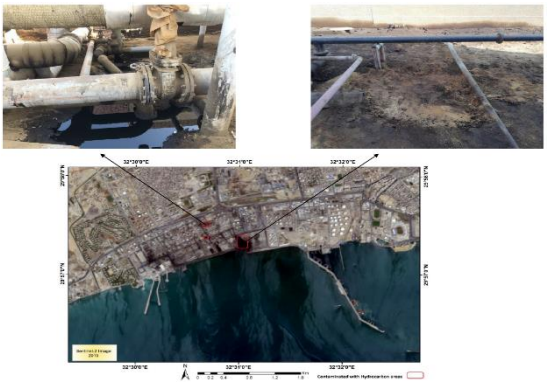

Figure 5 Site images showed contaminated soil inside Suez refinery plant (Hydrocarbons at liquid phase & mixed with soil phase, using Sentinel-2 in 2015).

Data processing workflow included pre-processing, processing, accuracy assessment, and integration with field data. Pre-processing involved radiometric calibration to convert digital numbers (DN) to top-of-atmosphere (TOA) spectral radiance. This was achieved by multiplying corrected image pixels by the calibration factor and dividing by the effective bandwidth.

Accuracy assessment employed a confusion matrix, a table with reference (observed) class categories as columns and classified (mapped) categories as rows. Each cell represents the number of observations mapped to a particular category that were actually observed in a different category. Diagonal cells indicate agreement between the map and ground truth, while off-diagonal cells represent misclassifications ([16]; [17]; [18]).

Then by using confusion matrix data Kappa statistics were calculated to show the difference between actual agreement and the agreement expected by chance [19].

$$K = \frac{observed\ \ accuracy\ -chance\ \ agreement}{1-chance\ \ agreement}$$

Results and Discussion

This study compared Sentinel-2 and Planetscope images to assess their suitability for precisely identifying contaminated soil (Figure 6). The results revealed that Sentinel-2's superior multispectral capabilities make it more sensitive to identifying oil spills compared to the Planetscope sensor.

Sentinel-2 observations from 2015 to 2021 were used to analyse changes in the intensity of darkness in potentially contaminated areas, revealing a peak in the year 2021. These observations also captured variations in sea colour across different locations, reflecting changes over time potentially resulting from oil leak activities in the gulf (Figure 7).

Figure 6 Planetscope and Sentinel-2 images of El Suez refinery plant in 2021 showed the high resolution of PlanetScope over Sentinel-2 to select ROIs and produce clustering map.

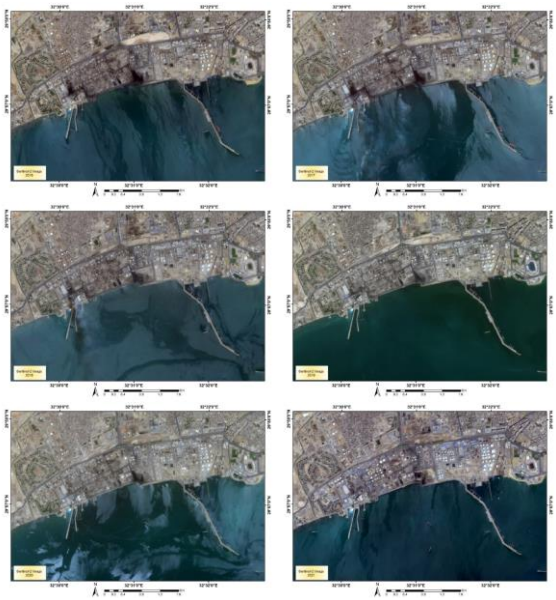

Figure 7 Sentinel-2 image of Suez refinery plant from 2016 to 2021.

Two samples each of contaminated and bare soil were collected and their spectral signatures were measured at the NARSS laboratory using an ASD Field Spec 4 instrument (Table 2). The resulting spectra are plotted in (Figure 8). These results were compared with those of Asadzadeh and de Souza Filho [10] and Correa Pabón, Souza Filho and Oliveira [20] in (Figure 9). Consistent with previous research, our spectra revealed distinct hydrocarbon absorption features at 1700nm (indicated with arrows). This feature, along with absorptions at other wavelengths, is characterized by a sharp left-side shoulder and a broader right-side shoulder, making the 1700nm wavelength the most reliable indicator of hydrocarbon contamination.

Additionally, These curves show that reflectance generally decreases as soil pollution increases. Heavily contaminated soil exhibits nearly constant reflectance across the entire wavelength range, while unpolluted soils have higher reflectance. This analysis reveals a correlation between reflectance value and soil type, suggesting the possibility of estimating soil oil pollution levels based on reflectance data. The current findings align with those of Orlov et al. [21]. Zawrah et al. [14] succeeded to estimate the organic hydrocarbons that threaten shallow Quaternary sandy aquifer Northwestern Gulf of Suez, Egypt using gas chromatography (GC). Samples were collected from Suez Refinery plant in Suez. According to Richard O. Gilbert [22] and Abdel-Moghny et al. [13], using an American auger, with total samples reach 40 samples from 8 different points, between 29° 57′ 33″ N and 32° 30′ 40′′ E, covering (1/15) of the total polluted area. Total petroleum hydrocarbon (TPH) extracted from eight samples then analyzed using gas chromatograph and data consisting of carbon distribution and percentage of paraffines for each sample were acquired. Sources can vary between vandalism, equipment failures, or accidents that cause direct pollution or discharge into the gulf and soil surface, [14].

Snousy et al. [15] recently conducted a study on micropollutants spread and movement behaviour through heterogeneous environment of Suez Gulf and found that dense anthropogenic activities particularly petroleum processing cause huge damage to ecosystem. Mixed pollutants like Fe, Pb, HOCs were found with high concentrations which may lead to degradation of environmental quality and chain of negative impacts on the environment

Table 2 samples collected from the studied site.

Sample description	Lattitude	Longitude	Photos captured for soil samples
Contaminated sample 1	29.95451	32.52889	A.
Contaminated sample 2	29.95451	32.52889	
Bare soil sample 1	29.9616	32.51165	B.
Bare soil sample 2	29.9616	32.51165	

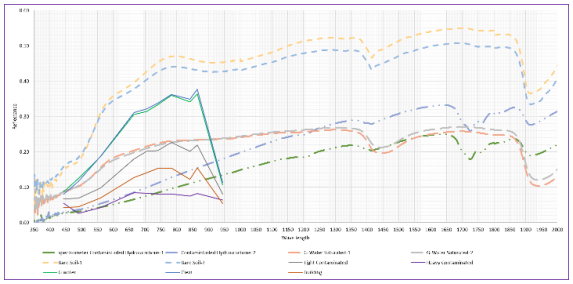

Figure 8 Reflectance spectra of collected soil samples, measured in NARSS laboratory using ASD Field Spec 4 instrument, by authors,

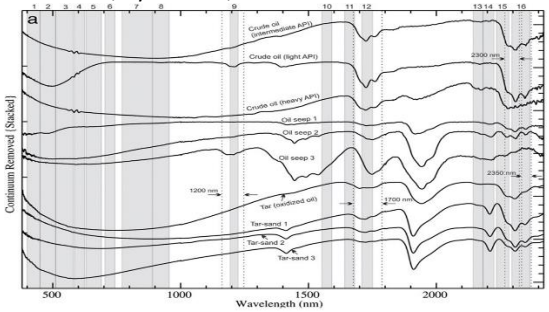

Figure 9 Reflectance spectra of HC-bearing compounds acquired from a variety of samples from Iran and Brazil, after Asadzadeh & de Souza Filho, (2016),

Supervised classification results from 2015 to 2021 reveal various land and water classes within the study area (Figure 10). The Suez Refinery Plant covers approximately 3.250 km2. Georeferenced data pinpoints contamination as red areas concentrated around storage tanks and pipelines within the plant. This contamination has increased from 2016 to the present day, indicated by the growth of the red polygon. While contamination decreased in 2017, red areas appeared in new locations within the plant for the first time. No significant changes were observed in 2018, but contaminated areas were reduced in 2019, likely due to soil replacement. In 2020 and 2021, contamination reached its peak, potentially linked to an increase in the refinery's production capacity.

During field investigations, thirty reference points were recorded for later use in validating the accuracy of the supervised classification map. The classified map's resulting classes were compared to the originally designated reference classes for each point, and this comparison was used to construct the classification table (Table 3). The overall accuracy of the map, considering all classed areas, was 83.33%, and the Kappa statistic (K) was 0.8. Notably, the detection accuracy for contaminated soil was 80%, indicating good results for identifying contaminated areas in the final map.

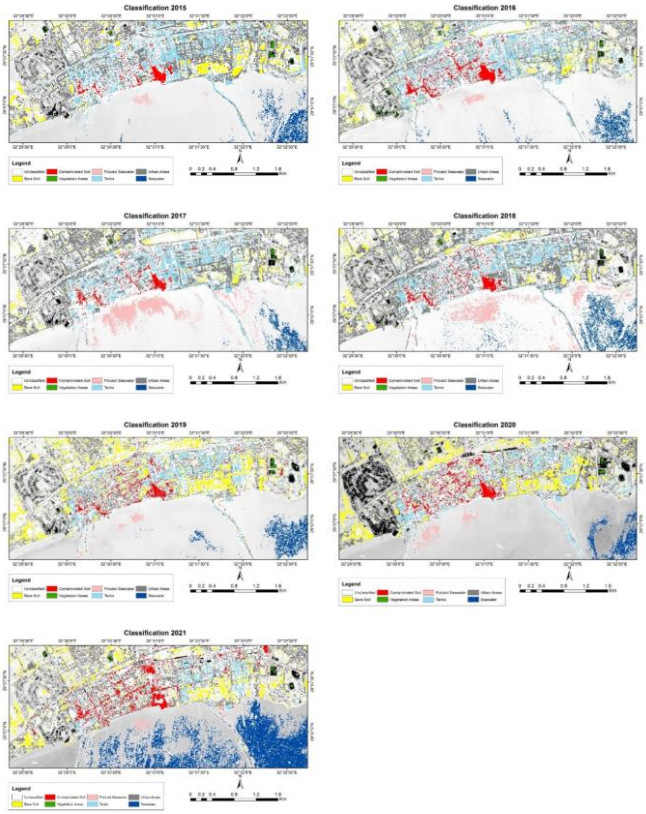

Figure 10 Supervised classification of Suez refinery plant from 2015 to 2021.

Table 3 Accuracy assessment table for the unused points.

Results \ Truth data	Bare soil	Cont_soil	green	Pol_water	tank	urban	water	Classification overall	User's accuracy (Precision)
Bare soil	2	0	0	0	0	0	0	2	100%
Cont_soil	0	4	0	0	0	0	0	3	100%
green	0	0	2	0	0	0	0	2	100%
Pol_water	0	0	0	3	0	0	0	3	100%
tank	0	0	0	0	4	0	0	4	100%
urban	4	1	0	0	0	6	0	11	54.54%
water	0	0	0	0	0	0	4	4	100%
Truth overall	6	5	2	3	4	6	4	30	
Producer's accuracy (Recall)	33.33%	80%	100%	100%	100%	100%	100%		
Overall accuracy (OA):								83.33%	
Kappa:								0.802	

Conclusion:

This study demonstrates the potential of remote sensing techniques, particularly Sentinel-2, for monitoring and mapping hydrocarbon-contaminated soil in urban coastal areas. Compared to traditional methods, these techniques offer advantages like rapid data acquisition, minimal sample preparation, and cost-effectiveness. The analysis of Sentinel-2 data from 2015 to 2021 revealed an increase in the intensity of darkness in potentially contaminated areas, potentially linked to oil leak activities. Additionally, the study confirmed the effectiveness of

spectral reflectance analysis in identifying hydrocarbon contamination, with the 1700nm wavelength proving most reliable. Furthermore, the supervised classification achieved an overall accuracy of 83.33% and a detection accuracy of 80% for contaminated soil, highlighting its potential for large-scale monitoring. This study revealed that contaminated soils with PHC were primarily located near pipelines and within deactivated land farms, suggesting industrial bioremediation techniques were previously used in these areas. The presence of hydrocarbon contamination in the Suez region was detected and confirmed using Sentinel-2 satellite spectral data. Ground truth validation demonstrated a strong correlation between maximum likelihood algorithm classification accuracy and field observations. The outlines of contaminated areas were successfully marked using the unique spectral patterns of contaminated soil. This evidence suggests potential hydrocarbon micro-seepage from Suez refinery plants. These findings highlight the effectiveness of remote sensing technologies for environmental monitoring and management in coastal regions, particularly for detecting and mapping hydrocarbon contamination.

Funding sources

This research received no external funding.

Conflicts of interest

Authors declare no conflict of interest.

Acknowledgment

The authors kindly acknowledge Planet Labs for supporting this research with its high spatial resolution satellite data (Planetscope). They also would like to acknowledge National Authority for Remote Sensing Society (NARSS) for allowing them to use the facilities of Big data lab.

References

[1] Noomen, M. F., Skidmore, A. K., van der Meer, F. D., & Prins, H. H. T. (2006). Continuum removed band depth analysis for detecting the effects of natural gas, methane, and ethane on maize reflectance. *Remote Sensing of Environment, 105*(3), 262–270. https://doi.org/10.1016/j.rse.2006.07.009

[2] Kolokoussis, P., & Karathanassi, V. (2018). Oil spill detection and mapping using Sentinel 2 imagery. *Journal of Marine Science and Engineering, 6*(1), 4. https://doi.org/10.3390/jmse6010004

[3] Grauer-Gray, J., & Hartemink, A. E. (2018). Raster sampling of soil profiles. *Geoderma, 318*, 99–108. https://doi.org/10.1016/j.geoderma.2017.12.029

[4] Weindorf, D. C., Bakr, N., & Zhu, Y. (2014). Advances in portable X-ray fluorescence (PXRF) for environmental, pedological, and agronomic applications. *Advances in Agronomy, 128*, 1–45. https://doi.org/10.1016/B978-0-12-802139-2.00001-9

[5] Xie, X. L., Pan, X. Z., & Sun, B. (2012). Visible and near-infrared diffuse reflectance spectroscopy for prediction of soil properties near a copper smelter. *Pedosphere, 22*(3), 351–366. https://doi.org/10.1016/S1002-0160(12)60022-8

[6] Ud din, S., Al Dousari, A., & Literathy, P. (2008). Evidence of hydrocarbon contamination from the Burgan oil field, Kuwait—Interpretations from thermal remote sensing data. *Journal of Environmental Management, 86*(4), 605–615. https://doi.org/10.1016/j.jenvman.2006.12.028

[7] Elachi, C., & van Zyl, J. (2006). Introduction. In *Introduction to the Physics and Techniques of Remote Sensing* (pp. 1–21). John Wiley & Sons, Inc. https://doi.org/10.1002/0471783390.ch1

[8] Mulder, V. L., de Bruin, S., Schaepman, M. E., & Mayr, T. R. (2011). The use of remote sensing in soil and terrain mapping: A review. *Geoderma, 162*(1–2), 1–19. https://doi.org/10.1016/j.geoderma.2010.12.018

[9] Management, R. E. (2008). State of oil pollution and management in (Vol. 2, July).

[10] Asadzadeh, S., & de Souza Filho, C. R. (2016). Investigating the capability of WorldView-3 superspectral data for direct hydrocarbon detection. *Remote Sensing of Environment, 173*, 162–173. https://doi.org/10.1016/j.rse.2015.11.030

[11] Wu, Y., et al. (2007). A mechanism study of reflectance spectroscopy for investigating heavy metals in soils. *Soil Science Society of America Journal, 71*(3), 918–926. https://doi.org/10.2136/SSSAJ2006.0285

[12] Youssef, Y. M., et al. (2021). Natural and anthropogenic coastal environmental hazards: An integrated remote sensing, GIS, and geophysical-based approach. *Surveys in Geophysics, 42*(5), 1109–1141. https://doi.org/10.1007/s10712-021-09660-6

[13] Abdel-Moghny, T., Mohamed, R. S. A., El-Sayed, E., Mohammed Aly, S., & Snousy, M. G. (2012). Effect of soil texture on remediation of hydrocarbons-contaminated soil at El-Minia District, Upper Egypt. *ISRN Chemical Engineering, 2012*, 1–13. https://doi.org/10.5402/2012/406598

[14] Zawrah, M., Ebiad, M., Rashad, A., & Snousy, M. G. (2014). GC estimation of organic hydrocarbons that threaten shallow Quaternary sandy aquifer Northwestern Gulf of Suez, Egypt. *Environmental Monitoring and Assessment*, 1–14. https://doi.org/10.1007/s10661-014-3949-5

[15] Snousy, M. G., Rashad, A. M., Ebiad, M. A. E. S., Helmy, H. M., & Abd El Bassier, M. A. (2018). Lead and associated micropollutant propagations in the North Suez Gulf, Egypt. *International Journal of Environmental Research, 12*(3), 357–371. https://doi.org/10.1007/s41742-018-0094-y

[16] Cohen, J. (2016). A coefficient of agreement for nominal scales. *Educational and Psychological Measurement, 20*(1), 37–46. https://doi.org/10.1177/001316446002000104

[17] Congalton, R. G. (1991). A review of assessing the accuracy of classifications of remotely sensed data. *Remote Sensing of Environment, 37*(1), 35–46. https://doi.org/10.1016/0034-4257(91)90048-B

[18] Noomen, M. F., Skidmore, A. K., van der Meer, F. D., & Prins, H. H. T. (2006). Continuum removed band depth analysis for detecting the effects of natural gas, methane, and ethane on maize reflectance. *Remote Sensing of Environment, 105*(3), 262–270. https://doi.org/10.1016/j.rse.2006.07.009

[19] Denniss, A. (1995). T. M. Lillesand & R. W. Kiefer, 1994. Remote sensing and image interpretation (3rd

ed.). *Geological Magazine, 132*(2), 248–249. https://doi.org/10.1017/S0016756800012024

[20] Correa Pabón, R. E., de Souza Filho, C. R., & de Oliveira, W. J. (2019). Reflectance and imaging spectroscopy applied to detection of petroleum hydrocarbon pollution in bare soils. *Science of the Total Environment, 649*, 1224–1236. https://doi.org/10.1016/j.scitotenv.2018.08.231

[21] Orlov, D. S., Ammosova, Y. A. M., Bocharnikova, Y. E. A., & Lopukhina, O. V. (1991). The use of reflectance of oil-polluted soils in monitoring from remote sensing imagery. *Mapping Sciences and Remote Sensing, 28*(4), 270–275. https://doi.org/10.1080/07493878.1991.10641876

[22] Gilbert, R. O. (1987). *Statistical methods for environmental pollution monitoring* (Book). OSTI.GOV. https://www.osti.gov/biblio/7037501-statistical-methods-environmental-pollution-monitoring